Bioelectrochromic hydrogel for fast antibiotic-susceptibility testing

Ferran Pujol-Vila[a]*, Jiri Dietvorst[b], Laura Gall-Mas[a], María Díaz-González[b], Núria Vigués[a], Jordi Mas[a], Xavier Muñoz-Berbel[b]

[a] Department of Genetics and Microbiology, Universitat Autònoma de Barcelona (UAB), Bellaterra, Barcelona, Spain
[b] Centre Nacional de Microelectrònica (IMB-CNM, CSIC), Bellaterra, Barcelona, Spain

Keywords: antibiotic-resistance determination, bioelectrochromic iron (III)/alginate hydrogel, electrodepositable material, Prussian Blue formation, metabolic chromatic response.

Materials science offers new perspectives in the clinical analysis of antimicrobial sensitivity providing materials of high and fast responsivity to environmental factors. However, biomaterial with capacity to respond to living bacteria has not been developed to date. We present an electrochromic iron(III)-complexed alginate hydrogel sensitive to bacterial metabolism, here applied to fast antibiotic-susceptibility determination. Bacteria under evaluation are entrapped –and pre-concentrated- in the hydrogel matrix by oxidation of iron (II) ions to iron (III) and in situ formation of the alginate hydrogel in less than 2 minutes and in soft experimental conditions (i.e. room temperature, pH 7, aqueous solution). After incubation with the antibiotic (10 minutes), ferricyanide is added to the biomaterial. Bacteria resistant to the antibiotic dose remain alive and reduce ferricyanide to ferrocyanide, which reacts with the iron (III) ions in the hydrogel to produce Prussian Blue molecules. For a bacterial

concentration above 10^7 colony forming units per mL colour development is detectable with the bare eye in less than 20 min. The simplicity, sensitivity, low-cost and short response time of the biomaterial and the assay envisages a high impact of these approaches on sensitive sectors such as public health system, food and beverage industries or environmental monitoring.

1. Introduction

Infectious diseases are still one of the main causes of health complications and dead worldwide [1]. The reasons for that have been identified and associated to the loose of effectiveness of traditional antimicrobial treatments and the emergence of multidrug resistant bacterial strains [2,3]. Personalized medicine, with person-specific treatments adapted to the infection of each patient, is envisioned as the most promising alternative to confront these limitations. The implementation of such strategies is limited by the characteristics of contemporary antimicrobial susceptibility tests [4]. These tests are based on culturing methods and require between 18 and 48 hours to provide a result, which postpones medical decisions and the beginning of the treatment. The delay in the treatment and the bad selection of the antibiotic type or dose are responsible of most of bad prognostic and deaths related to infectious diseases.

In this context, material science is taking advantage of new biomaterials formulations and the versatility of their synthetic routes to impact on several fields, also on clinical analysis . Much attention has been paid to the development of the so-called stimuli-responsive biopolymers (SRBP) [6], bio-macromolecular systems experiencing significant physic-chemical changes in response to external environmental conditions. Typical external stimuli include environmental factors such as pH [7], temperature [8],

and electrolyte concentration [9] or the application of electric, magnetic, sonic and electromagnetic (photo/light) fields [10,11,9]. Based on the latter, biomaterials with improved properties as scaffolds for tissue engineering [12,13] or regenerative medicine [14,15], drug encapsulation and selective delivery in response to external stimuli [16], as well as sensors or actuators [6] have been already described. As a step forward, biologically-responsive biopolymers (BRBP) are designed to respond to stimuli inherently present in natural systems [17,18].On the basis of this concept, BRBP sensitive to glucose (glucose-responsive polymers) [19], the activity of enzymes (enzyme-responsive polymers) [20] and selective biomolecules present in the natural environment (antigen-responsive polymers) [21] have been already developed. However, to the best of our knowledge, a BRBP with capacity to evaluate antimicrobial susceptibility of bacterial isolates and to identify resistant strains has not been reported yet.

With the aim to adapt antimicrobial susceptibility tests to the current requirements of personalized medicine, we have developed an electrodepositable iron (III)/alginate biomaterial, with capacity to retain (and pre-concentrate) bacteria as well as sensitivity for fast evaluation of antimicrobial susceptibility (and resistance) to antibiotics. Antimicrobial susceptibility/resistance tests with the biomaterial involved three steps: (i) bacterial entrapment in the iron(III)-alginate hydrogel by electrodeposition at soft reaction conditions (i.e. room temperature, aqueous solutions, pH 7), (ii) incubation with the antibiotic (10 minutes) and (iii) colour development after incubation with ferricyanide (20 minutes), enabling the determination of antibiotic susceptibility in 30 minutes and by simple visual inspection. Electrodeposition and sensing protocols are evaluated and optimized in the manuscript. The final biomaterial is validated using *Escherichia coli* and *Staphylococcus aureus* strains sensitive and resistant to kanamycin.

2. Experimental section

2.1. Chemical reagents

All chemicals were of analytical grade and all solutions were prepared in distilled water, unless otherwise stated**.** Sodium alginate, potassium ferrocyanide and potassium ferricyanide were purchased from Sigma-Aldrich (US). Iron (III) chloride, iron (II) sulphate, sodium chloride, ascorbic acid, Kmc and glucose were purchased from Panreac (Spain).

2.2. Hydrogel fabrication by direct gelation

Direct gelation was carried out by addition of iron (III) chloride solutions to sodium alginate samples at room temperature. Alginate and iron (III) final concentrations in the hydrogel were 0.5 % (w/v) and 30 mM, respectively. For bacterial hydrogel fabrication, bacterial suspension in 0.9 % (w/v) sodium chloride was mixed with alginate solution and gelation was carried out as previously. After gelation, excess liquid was removed and hydrogels were washed 3 times with 0.9 % (w/v) sodium chloride to remove non-gelled alginate, residual iron (III) and non-entrapped bacteria (if present).

2.3. Hydrogel fabrication by electrodeposition

An aqueous solution composed of sodium alginate and iron (II) sulphate was dropped on screen-printed carbon electrodes (Dropsens, Oviedo, Spain). Electrodeposition of the hydrogel was achieved by potentiostatic oxidation of iron (II) ions to iron (III) at 1.2 V (vs Ag presudoreference) with a multichannel potentiostat driven by Dropview software (Dropsens, Oviedo, Spain). For bacterial hydrogel electrodeposition, bacterial suspension in 0.9 % (w/v) sodium chloride was mixed with alginate and iron (II)

sulphate solution, and electrodeposited as before. Prior to hydrogel analysis, excess liquid was removed and hydrogels were washed 3 times with 0.9 % (w/v) sodium chloride to remove iron, alginate and bacterial residues.

2.4. Hydrogel characterization

Optical measurements were carried out in an optical setup already reported [23].The setup consisted of a poly(methyl methacrylate) (PMMA) cuvette with a 120-µL reservoir for alginate hydrogel formation and two 230 µm multimode optical fibers (Thorlabs, Dachau, Germany) coupled to it. Optical fibers were located and aligned on both sides of the PMMA structure (optical path = 1.6 cm) and respectively connected to the emitter, i.e. a halogen/deuterium light source (DH-2000 UV-VIS-NIR Light Source, Ocean Optics, Florida, US), and to the detector (USB2000 + XR microespectrometer, Ocean Optics, Florida, US). SpectraSuite software (Ocean Optics, USA) was used for data acquisition. Hydrogels were fabricated in situ on the cuvette reservoir by the previous protocol. For hydrogels fabricated in 96-well plates optical measurements were carried out using a microplate reader (Thermo-Fisher).

Hydrogel thickness was measured with an optical profilometer (PLµ 2300, Sensofar-Tech, Spain) and image analysis by PLµ Confocal Imaging Profiler software (Sensofar-Tech, Spain).

Cell viability in bacterial hydrogels was assessed by staining with Live/Dead Invitrogen Kit Bac Light (Invitrogen) by following the protocol detailed by the supplier. Stained hydrogels were visualized with a Zeiss AXIO Imager A1 fluorescence microscope (Zeiss, Oberkochen, Germany) and Laser Confocal Leica TCS SP2 AOBS (Leica, Heidelberg, Germany) from the Servei de Microscopia at UAB. Imaris software was used for 3D constructions.

2.5. Bacteria cultivation and preparation

E. coli K12 (CGSC 5073) and *Staphylococcus aureus* (ATCC 6538) were grown aerobically for 18 h at 37 ºC in Luria-Bertani (LB) broth, centrifuged at 10100 x g 15 min and resuspended in 0.9 % (w/v) sodium chloride. Cell concentration was determined by absorbance measurement at 600 nm.

3. Results and discussion

3.1. Biomaterial electrodeposition and cell entrapment

Alginate present ideal functional and structural properties as cell support and intrinsic responsivity, derived from its huge versatility [22]. An alginate concentration of 0.5% was selected according to bibliography [23] to ensure homogeneity, cell entrapment capacity and stability. From the myriad of gelling agents, iron (III) ions were chosen for enabling hydrogel electron-mediated deposition and sensitivity to redox species. Electrodeposition is very valuable for enabling: (i) control of the deposition process (ii) control of hydrogel properties (i.e. porosity, thickness, density, definition of the deposition area, among others), (iii) homogeneity and (iv) repeatability. Iron(III) /alginate hydrogels were prepared following the protocol detailed in [24]. Iron (II) ions were mixed with the alginate solution and in situ oxidized for local formation of the iron(III)/alginate hydrogels at very soft experimental conditions (i.e. room temperature, pH 7, aqueous solution). Thick hydrogel films were potentiostatically electrodeposited on the working electrode of screen-printed carbon electrodes (SPCEs; **Figure 1a**). A potential of 1.2 V (vs Ag) was chosen from iron (II) sulphate cyclic voltammetry data (**Figure 1a** inset), as the lowest potential allowing iron (II) oxidation and hydrogel formation. As shown in **Figure 1b**, electrodeposition enabled the definition of the

deposition area with high precision, generating hydrogels with very vertical walls. Optimal iron (II) sulphate concentration and electrodeposition times were selected from hydrogel thickness (from profilometry) and chronoamperometry data. Thicker hydrogels were obtained when increasing either the iron (II) concentration in the sample (**Figure 1c**) or the electrodeposition time (**Figure 1d**) up to stabilization at values around 60 mM iron (II) and 450 - 500 s, respectively. The thickness of the hydrogel, however, also affected ferricyanide diffusion. Chronoamperometry data shows important current limitation by hydrogels containing more than 20 mM iron (**Figure 1e**), which corresponded to thicknesses above 100 μm. Diffusion was, however, less affected by the electrodeposition time (**Figure 1f**) since the influence of this parameter to the hydrogel thickness was lower. Electrodeposition at 1.2 V (vs Ag) of 20 mM iron (II) samples for 500 s, providing hydrogels of around 100 μm was selected for further experiments.

High bacterial densities were entrapped in the 3D matrix of the alginate hydrogel biomaterial, without compromising cell integrity or activity. It is clear in the live/dead stained hydrogel shown in **Figure 2a**, where most of entrapped cells present a green fluorescence indicative of the integrity of their plasmatic membrane and their viability (in opposition to red microorganisms which are non-viable). However, bacterial concentrations above $2.5 \cdot 10^8$ colony forming units per mL (CFU/mL) limited current flow and hydrogel formation (**Figure 2b**). This concentration was considered, therefore, as the highest bacterial concentration able to be electrodepositated. Ferricyanide concentration for the bioassay was adjusted to the number of immobilized bacteria. Based on previous works [25,26,27], ferricyanide concentration was set at 1 mM (for a hydrogel containing $2.5 \cdot 10^8$ CFU/mL) with the objective to ensure a sensitive response of the biomaterial in less than one hour.

3.2. Electrochromic response of the biomaterial

The presence of iron (III) ions in the hydrogel provides the biomaterial with redox activity and reactivity. This reactivity is exploited in the development of a biomaterial with sensitivity to bacterial metabolism, reporting on bacterial susceptibility to antibiotics and antibiotic resistance. The sensing principle of the biomaterial takes benefit from the selective reactivity of iron (III)/alginate hydrogels to hexacyanoferrate molecules, which is illustrated in **Figure 3a**. As shown, the biomaterial was not sensitive to the presence of ferricyanide, while it reacted with ferrocyanide producing an intense blue colour as a result of PB nanoparticles formation. This selective reactivity is clearly demonstrated by spectrometric analysis of the hydrogels. After addition of ferricyanide, an intense absorption band at 420 nm appears in the hydrogel by the presence of ferricyanide molecules (**Figure 3b**). The absorption band of ferricyanide, however, remained stable over time, which confirmed the low reactivity of this reagent with the biomaterial. Ferrocyanide, on the other hand, reacted with the biomaterial, producing PB nanoparticles with an intense absorption band at 680 nm (**Figure 3c**). The increase in the absorbance magnitude at 680 nm (Abs_{680}) over time reported on the PB formation kinetics. After 30 minutes, Abs_{680} reached a maximum indicating the end of the reaction under this experimental conditions.

The formation of PB molecules depended on the initial concentration of ferrocyanide, being either directly added to the biomaterial (**Figure 3d**) or in situ generated by reduction of ferricyanide with ascorbic acid (**Figure 3e**). Biomaterial reactivity after direct addition and in situ formation of ferrocyanide was compared. To allow comparison, the stoichiometry of the reduction reaction, where one molecule of ascorbic acid reduced two molecules of ferricyanide, was considered. In both cases, similar

results were obtained after 30 minutes of reaction with the biomaterial (**Figure 3g**). Minor differences were observed in the saturation region, mostly due to kinetic limitations of the reduction reaction [28]. Therefore, the biomaterial was also sensitive to processes involving the reduction of ferricyanide.

3.3. Electrochromic sensing of bacterial metabolism with the biomaterial

Ferricyanide, and other electrochromic molecules, present high redox potentials and can report on bacterial metabolism by the mechanisms summarized below [25]. Bacteria oxidize nutrients to obtain energy. In this process, they generate an electron flow in the cell membrane through a number of proteins known as electron transfer chain. This chain of coupled proteins transfers the electrons to a final electron acceptor, oxygen in the case of aerobic metabolism. However, due to its redox potential, oxygen may be replaced by a suitable electrochromic molecule such as ferricyanide, which is metabolically reduced to ferrocyanide. Since the reduction is directly linked to bacterial metabolism, only living bacteria (and not dead ones) can produce ferricyanide reduction. The metabolic reduction of ferricyanide is here employed in the development of a biomaterial for fast antibiotic susceptibility testing.

First, bacteria were entrapped in the alginate matrix by electrodeposition with the previous protocol. Due to the iron complexation in the matrix**,** entrapped bacteria could not reduce iron (III) ions directly, ensuring the integrity and stability of the biomaterial. **Figure 4a** schematizes the sensing mechanism of the biomaterial, where only living bacteria, and not dead ones, reduce ferricyanide to ferrocyanide inducing PB formation and the consequent change of colour. The response of the biomaterial containing $2.5 \cdot 10^8$ CFU mL^{-1} of *Escherichia coli* (*E. coli*, used as model bacterium) to the addition of 1 mM ferricyanide solution is illustrated in **Figure 4b**. The presence of bacteria in the hydrogel increased absorbance due to cell scattering. Apart from scattering,

absorption bands corresponding to ferricyanide (420 nm) and PB (680 nm) were clearly identified. Spectrometric changes in the sensing biomaterial were mostly due to the formation of blue-coloured PB, while ferricyanide reduction was difficult to appreciate. The increase in Abs_{680} was fast and only required 30 - 35 minutes to reach a maximum in the absorbance magnitude. However, the sensitivity (slope in the curve) was smaller than that obtained by direct addition of ferrocyanide due to kinetic limitations of bacterial metabolism (**Figure 4c**). Even though, the biomaterial was able to provide quantitative data after short time periods.

Due to the metabolic nature of the electrochromic reaction in the biomaterial, the response of the hydrogel was subjected to the influence of environmental factors affecting bacterial activity such as metabolic stimulators (e.g. nutrients) or inhibitors (e.g. toxic agents). This modulation of metabolic activity was evaluated using glucose as stimulator and ethanol as inhibitor. **Figure 5a** shows the absorbance spectra of hydrogels incubated with samples containing different glucose concentrations. After 30 minutes of incubation, PB formation, measured as Abs_{680nm}, presented a high dependence on the concentration of glucose in the sample up to saturation around 0.05% (w/v), while no significant changes were observed in the absorbance band corresponding to ferricyanide, Abs_{420nm} (**Figure 5b** and **5c**). The presence of ethanol influenced the absorbance spectrum of the biomaterial (**Figure 5d**). In this case, ethanol reduced the metabolic activity and viability of cells, and consequently the PB formation. As before, most of the chromatic change recorded was associated to PB (**Figure 5e**), demonstrating the enhancement of sensitivity when coupling ferricyanide reduction to PB formation. There was a clear relationship between metabolic activity inhibition and the concentration of ethanol in the sample, reaching 100% inhibition by values around 10% (v/v) of ethanol (**Figure 5f**). These results validated the use of this biomaterial for

fast and sensitive determination of bacterial activity and viability, as well as bacterial susceptibility to toxic agents such as ethanol.

3.4. Antibiotic susceptibility testing with the electrochromic biomaterial

As a step forward, the biomaterial was finally applied to fast and simple antibiotic susceptibility testing. To this end, kanamycin (Kmc) was chosen as antimicrobial agent. High bacterial concentrations (i.e. $2.5 \cdot 10^8$ CFU mL^{-1}) of the strains under study (in this case *E. coli* sensitive and *S. aureus* resistant to Kmc antibiotic) were entrapped in the hydrogel matrix by direct gelation in 96-well plates. The susceptibility of these two strains to Kmc was previously characterized showing sensitivity in *E. coli* and resistance in *S. aureus* for the tested antibiotic concentrations (from 1 to 128 mg L^{-1}). The biomaterial was then incubated with Kmc concentrations between 1 and 128 mg/L for 30 minutes, rinsed with distilled water and incubated with 1 mM ferricyanide for inducing the electrochromic response. The images of the biomaterials with resistant (RS) and non-resistant strains (NRS) at different incubation times are shown in **Figure 6a**. From the images it is clear that there was a big difference between biomaterials containing NRS, which remained yellow for the presence of ferricyanide, and RS, which started developing blue colour (due to PB formation) even after only 5 minutes of incubation. With time, these differences between RS and NRS were accentuating since the colour in the RS increased colour depth. At this antibiotic dose range, RS were completely resistant and no significant differences were observed. NRS, on the other hand, presented a dose-dependence on the antibiotic concentration range under study. Images in **Figure 6a** show how there was a delay in colour development even in the sample that did not contain antibiotic (labelled as 0). This may be due to differences in the metabolic state or concentration of both strains. However, sample 0 and 1, which

corresponds to a concentration of 1 mg/L of Kmc, presented a similar kinetic of blue colour development whereas samples containing 32 and 128 mg/L remained yellow. The same result was obtained when comparing the absorbance magnitude at 680 nm after 20 minutes of incubation with ferricyanide (**Figure 6b**), which confirmed that the half maximal inhibitory concentration (IC50) of this antibiotic for this bacterial strain should be between 1 and 32 mg/L. Control samples correspond to the biomaterial without bacteria.

According to these results, the electrodepositable iron(III)/alginate hydrogel here presented is ideal for fast and sensitive testing of antibacterial susceptibility and for the identification of bacterial resistance by a simple change of colour, which can be even perceptible with the bare eye (without the need of external instrumentation). The simplicity and versatility of the biomaterial and the sensing mechanism make this metabolic stimuli-sensitive material very interesting in a broad spectrum of applications, such as toxicity assessment, food quality control and clinical diagnosis.

4. Conclusions

In conclusion, we present an electrodepositable hydrogel biomaterial composed of iron (III) ions and alginate with a strong electrochromatic response to bacterial metabolism, here applied to the fast and sensitive determination of bacterial susceptibility to antibiotic, also enabling the identification of resistant bacterial strains. Bacteria under study are entrapped and pre-concentrated in the biomaterial by electrodeposition at soft reaction conditions (i.e. room temperature, aqueous solution, pH 7) without compromising bacterial integrity or activity. Electrodeposition ensures the repeatability and reproducibility of the assay. During incubation with ferricyanide, bacteria resistant to the antibiotic type or dose use this molecule as final electron acceptor and reduce it to

ferrocyanide. The in situ generated ferrocyanide reacts with iron (III) ions from the hydrogel producing PB molecules and an intense change of colour that can be detected with the bare eye in less than 30 minutes. Non-resistant bacterial strains present a dose-dependent response to the antibiotic which enables the determination of clinically relevant parameters such as the minimal inhibitory concentration or the half maximal inhibitory concentration. The biomaterial enables fast and sensitive determination of susceptibility to antibiotics and the identification of resistant strains, something of key relevance in the development of new protocols for personalized treatments and medicine. The impact of the current biomaterial, however, is not limited to this area of interest but it is envisaged to impact on other sectors where fast methods for microbial analysis are also required, such as environmental monitoring or the food and beverage industries.

Acknowledgements

F P-V wants to acknowledge to PIF fellowship from UAB. X. M-B was supported by the “Ramón y Cajal” program from the Spanish government. This work was partially funded by projects RTC-2016-5766-2, CTQ2014-54553-C3-2-R and CTQ2014-61809-EXP to JM with participation of the European Regional Development Fund (ERDF). This work was partially funded by the European Comission through the project ND4ID (H2020-MSCA-ITN-2015- 675412).

References

[1] Dye C. After 2015: infectious diseases in a new era of health and development. Philos Trans R Soc Lond B Biol Sci 2014;369: 1645: 20130426.

[2] Tegou E, Magana M, Katsogridaki AE, Ioannidis A, Raptis V, Jordan S, Chatzipanagiotou S. Chatzandroulis S. Ornelas C. Tegos GP. Terms of endaerment: Bacteria meet graphene nanosurfaces. Biomaterials 2016; 89:38-55.

[3] WHO Antimicrobial resistance. Global report of surveillance 2014. Geneva, 2014

[4] Reller LB, Weinstein M, Jorgensen JH, Ferraro MJ. Antimicrobial susceptibility testing: a review of general principles and contemporary practices. Clin Infect Dis 2009;49:1749-55.

[5] Hardy JG, Palma M, Wind SJ, Biggs MJ. Responsive Biomaterials: Advances in Materials Based on Shape-Memory Polymers. Adv Mater 2016;28:5717-24.

[6] Ferreira J, Girotto EM. Optical pH sensitive material based on bromophenol blue-doped polypirrole. Sens Actuator B-Chem 2009;137:426-31.

[7] Roy D, Brooks WLA, Sumerlin BS. New directions in thermoresponsive polymers.Chem Soc Rev 2013;*42*:7214-43.

[8] Roy D, Cambre JN, Sumerlin BS. Future perspectives and recent advances in stimuli-responsive materials. Prog Polym Sci 2010;35:278-301.

[9] Jochum FD, Theato P. Temperature- and light-responsive smart polymer materials. Chem Soc Rev 2013;*42*:7468-83.

[10] Ahn S, Kasi RM, Kim SC, Sharma N, Zhou Y. Stimuli-responsive polymer gels, Soft Matter 2008;*4*:1151-57.

[11] Peppas NA, Hilt JZ, Khademhosseini A, Langer R. Hydrogels in Biology and Medicine: From Molecular Principles to Bionanotechnology. Adv Mater 2006;*18*:1345-60.

[12] Van Vlierberghe S, Dubruel P, Schacht E, Biopolymer-Based Hydrogels As Scaffolds for Tissue Engineering Applications: A Review, Biomacromolecules 2011;*12*:1387-1408.

[13] Aguilar MR, Elvira C, Gallardo A, Vázquez B, Román JS. in Topics in Tissue Engineering, Vol. 3 (Eds: N. Ashammakhi, R. Reis, E. Chielini) Expertissues (Network of Excellence) 2007; Ch.6.

[14] Sun J, Tan H. Alginate-Based Biomaterials for Regenerative Medicine Applications. Materials 2013;*6*:1285-1309.

[15] Slaughter BV, Khurshid SS, Fisher OZ, Khademhosseini A, Peppas NA. Hydrogels in Regenerative Medicine. Adv Mater 2009;*21*:3307-29.

[16] Giammanco GE, Sosnofsky CT, Ostrowski AD. Light-responsive iron(III)-polysaccharide coordination hydrogels for controlled delivery, ACS Appl Mater Interfaces 2015;7:3068-76.

[17] Miyata T, Uragami T, Nakamae K, Biomolecule-sensitive hydrogels. Adv Drug Delivery Rev 2002; 54:79-98.

[18] Appel EA, Loh XJ, Jones ST, Biederman F, Dreiss CA, Sherman OA. Ultrahigh-Water-Content Supramolecular Hydrogels Exhibiting Multistimuli Responsiveness. J Am Chem Soc 2012; 11767-73.

[19] Ito Y, Casolaro M, Kono K, Imanishi Y. An insulin-releasing system that is responsive to glucose. J Control Release 1989;10:195-203.

[20] Ulijin RV. Enzyme-responsive materials: a new class of smart biomaterials. J Mater Chem 2006;16:2217-25.

[21] Lu Z, Kopeckova P, Kopecek J. Antigen responsive hydrogels based on polymerizable antibody Fab fragment. Macromol Biosci 2003;3:296-300.

[22] Machida-Sano I, Ogawa S, Ueda H, Kimura Y, Satoh N, Namiki H. Effects of Composition of Iron-Cross-Linked Alginate Hydrogels for Cultivation of Human Dermal Fibroblasts. Int J Biomater 2012;*8*20513.

[23] Sanahuja D, Giménez-Gómez P, Vigués N, Ackerman TN, Guerrero-Navarro AE, Pujol-Vila F, Sacristán J, Santamaria N, Sánchez-Contreras M, Díaz-González M, Mas J, Muñoz-Berbel X. Microbial trench-based optofluidic system for reagentless determination of phenolic compounds. Lab Chip 2015;15:1717-26.

[24] Jin Z, Güven G, Bocharova V, Halámek J, Tokarev I, Minko S, Melman A, Mandler D, Katz E. Electrochemically controlled drug-mimicking protein release from iron-alginate thin-films associated with an electrode, ACS Appl Mater Interfaces 2012;4:466-75.

[25] Pujol-Vila F, Vigués N, Díaz-González M, Muñoz-Berbel X, Mas J. Fast and sensitive optical toxicity bioassay based on dual wavelength analysis of bacterial ferricyanide reduction kinetics. Biosens Bioelectron 2015;*67*:272-79.

[26] Pujol-Vila F, Giménez-Gómez P, Santamaria N, Antúnez B, Vigués N, Díaz-González M, Jiménez-Jorquera C, Mas J, Sacristán J, Muñoz-Berbel X. Portable and

miniaturized optofluidic analysis system with ambient light correction for fast in situ determination of environmental pollution. Sens Actuator B-Chem 2016;*222*:55-62.

[27] Pujol-Vila F, Vigués N, Guerrero-Navarro AE, Jiménez S, Gómez D, Fernández M, Bori J, Vallès B, Riva MC, Muñoz-Berbel X, Mas J. Paper-based chromatic toxicity bioassay by analysis of bacterial ferricyanide reduction. Anal Chim Acta 2016;910:60-67.

[28] Mehrotra US, Agrawal MC, Mushran SP. Kinetics of the reduction of hexacyanoferrate(III) by ascorbic acid, J Phys Chem 1969;73:1996-99.

Figure 1

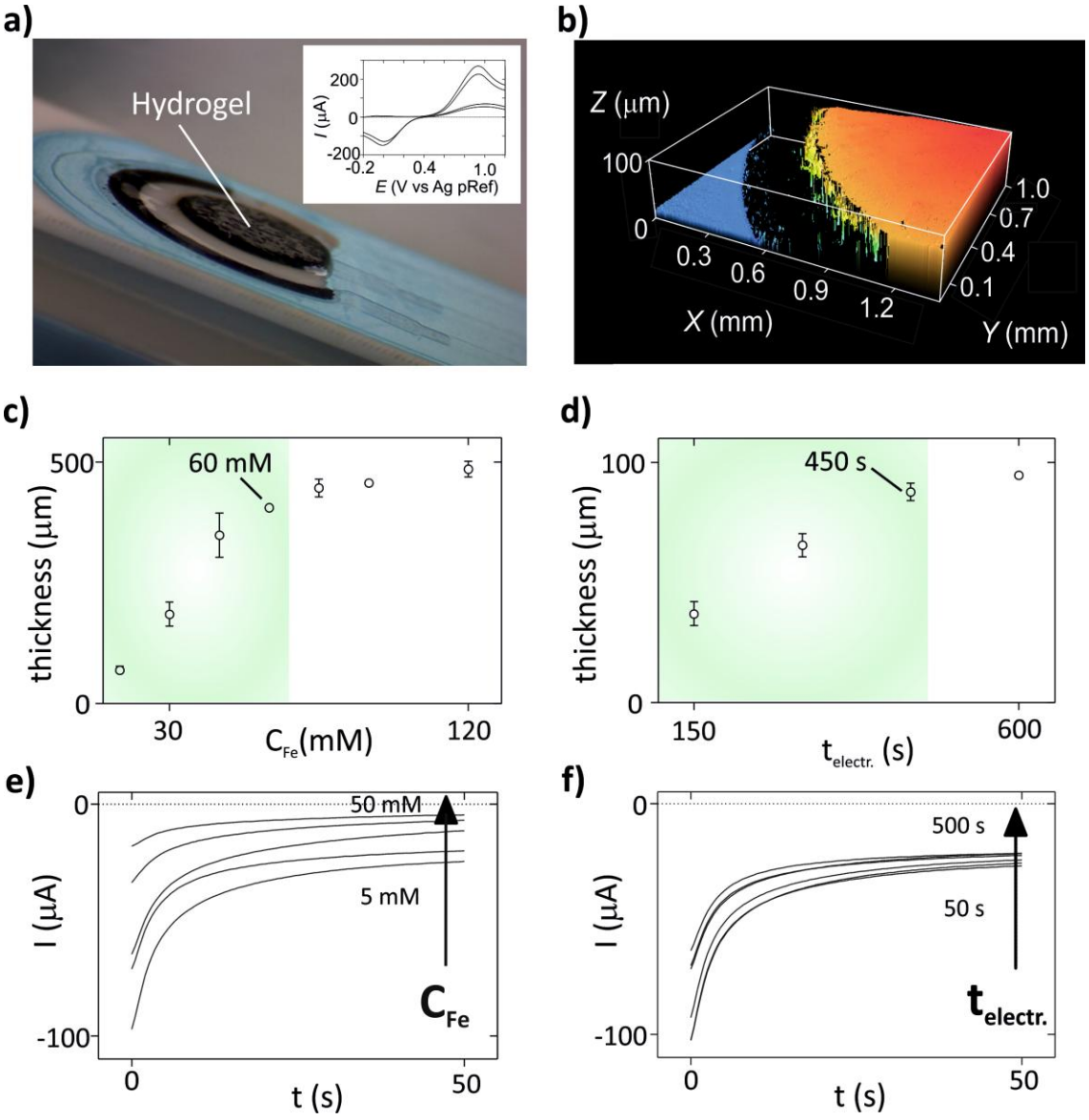
a)
Hydrogel
200
0
-200
I (µA)
-0.2
0.4
1.0
E (V vs Ag pRef)
b)
Z (µm)
100
0
0.3
0.6
0.9
1.2
X (mm)
1.0
0.7
0.4
0.1
Y (mm)
c)
500
0
thickness (µm)
60 mM
30
C_Fe(mM)
120
d)
100
0
thickness (µm)
450 s
150
t_electr. (s)
600
e)
0
-100
I (µA)
50 mM
5 mM
C_Fe
0
t (s)
50
f)
0
-100
I (µA)
500 s
50 s
t_electr.
0
t (s)
50

Figure 2

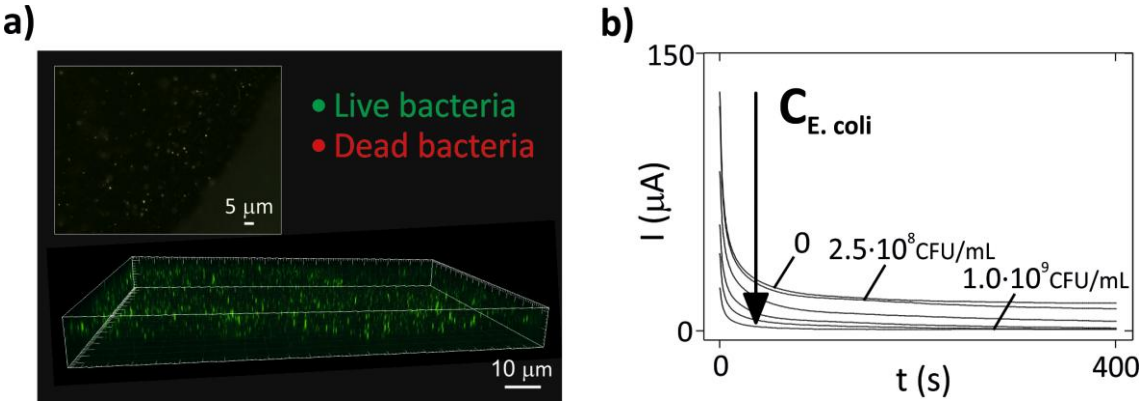
a)
Live bacteria
Dead bacteria
5 µm
10 µm
b)
150
0
I (µA)
$C_{E. coli}$
0
$2.5 \cdot 10^8$ CFU/mL
$1.0 \cdot 10^9$ CFU/mL
0
400
t (s)

Figure 3

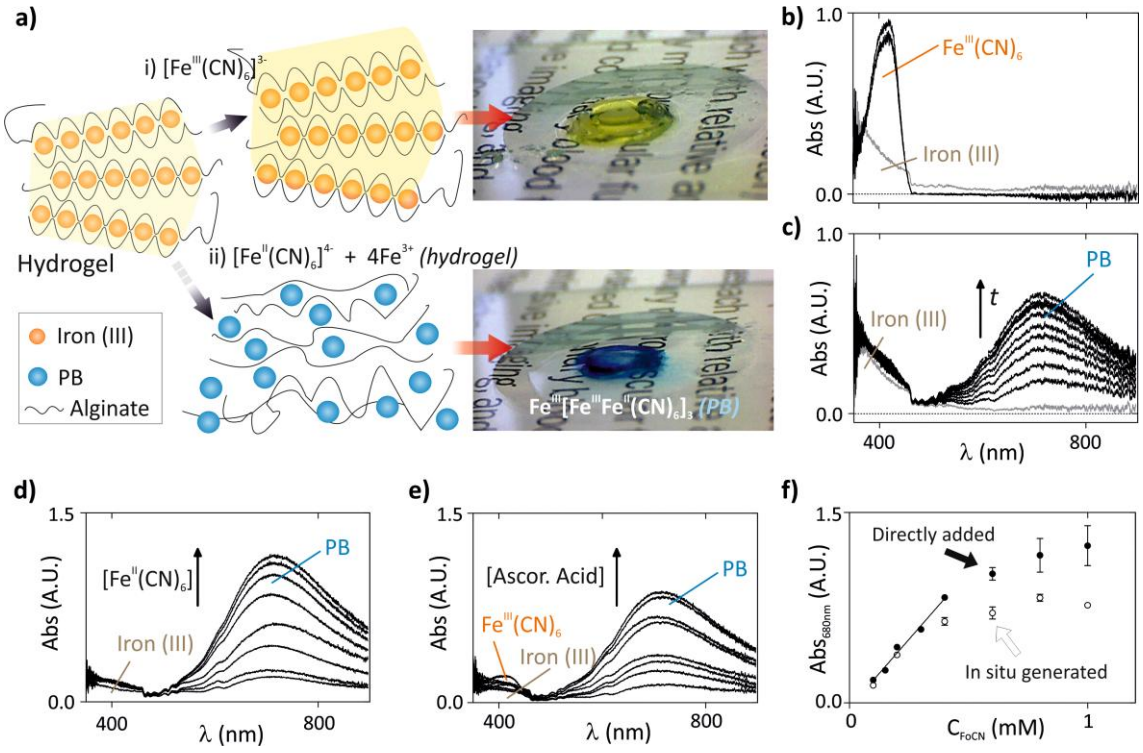
a)
i) [Fe^{III}(CN)$_6$]$^{3-}$
Hydrogel
ii) [Fe^{II}(CN)$_6$]$^{4-}$ + 4Fe^{3+} (hydrogel)
Iron (III)
PB
Alginate
Fe$^{III}_4$[Fe^{III}Fe^{II}(CN)$_6$]$_3$ (PB)
b)
Fe^{III}(CN)$_6$
Iron (III)
Abs (A.U.)
c)
PB
Iron (III)
t
λ (nm)
d)
[Fe^{II}(CN)$_6$]
PB
Iron (III)
e)
[Ascor. Acid]
PB
Fe^{III}(CN)$_6$
Iron (III)
f)
Directly added
In situ generated
Abs$_{680nm}$ (A.U.)
C$_{FoCN}$ (mM)

Figure 4

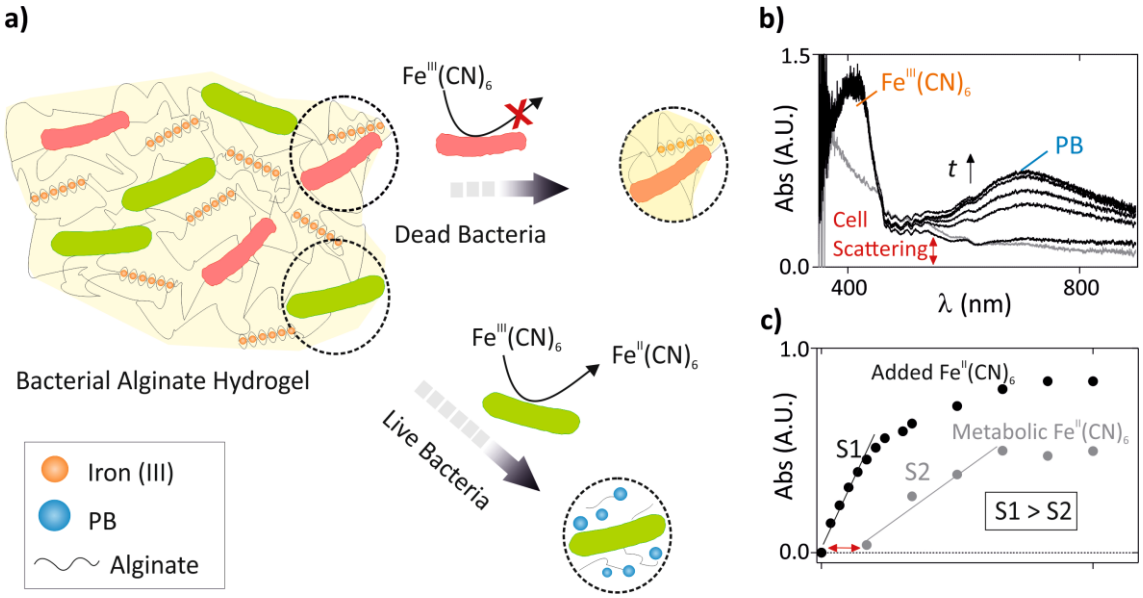
a)
$Fe^{III}(CN)_6$
Dead Bacteria
Bacterial Alginate Hydrogel
$Fe^{III}(CN)_6$
$Fe^{II}(CN)_6$
Live Bacteria
Iron (III)
PB
Alginate
b)
1.5
$Fe^{III}(CN)_6$
PB
t
Cell
Scattering
Abs (A.U.)
0.0
400
800
λ (nm)
c)
1.0
Added $Fe^{II}(CN)_6$
Metabolic $Fe^{II}(CN)_6$
S1
S2
S1 > S2
Abs (A.U.)
0.0

Figure 5

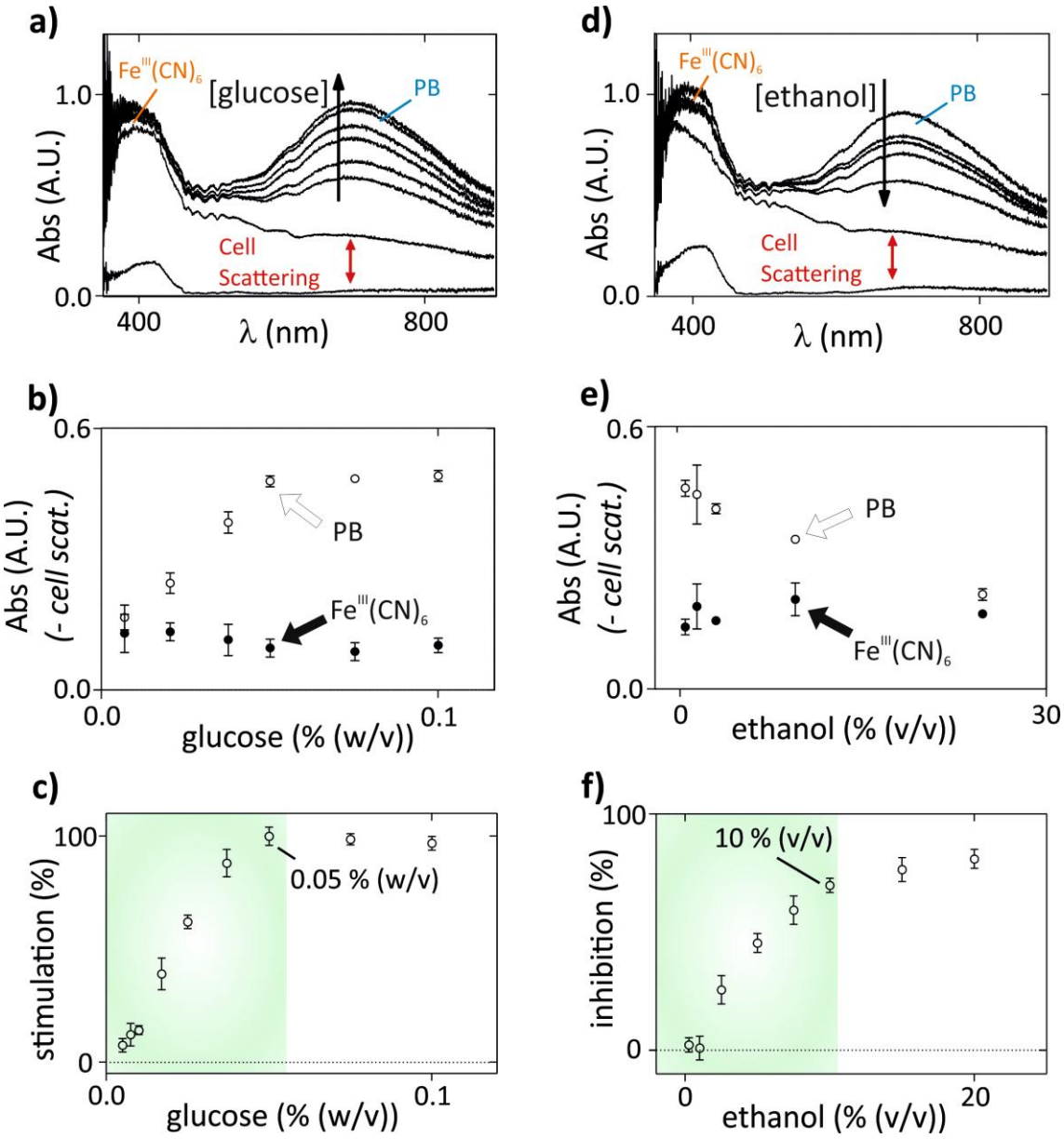
a)
Fe^{III}(CN)$_6$
[glucose]
PB
Abs (A.U.)
1.0
0.0
Cell
Scattering
400
λ (nm)
800
d)
Fe^{III}(CN)$_6$
[ethanol]
PB
Abs (A.U.)
1.0
0.0
Cell
Scattering
400
λ (nm)
800
b)
Abs (A.U.)
(- cell scat.)
0.6
0.0
PB
Fe^{III}(CN)$_6$
0.0
glucose (% (w/v))
0.1
e)
Abs (A.U.)
(- cell scat.)
0.6
0.0
PB
Fe^{III}(CN)$_6$
0
ethanol (% (v/v))
30
c)
stimulation (%)
100
0
0.05 % (w/v)
0.0
glucose (% (w/v))
0.1
f)
inhibition (%)
100
0
10 % (v/v)
0
ethanol (% (v/v))
20

Figure 6

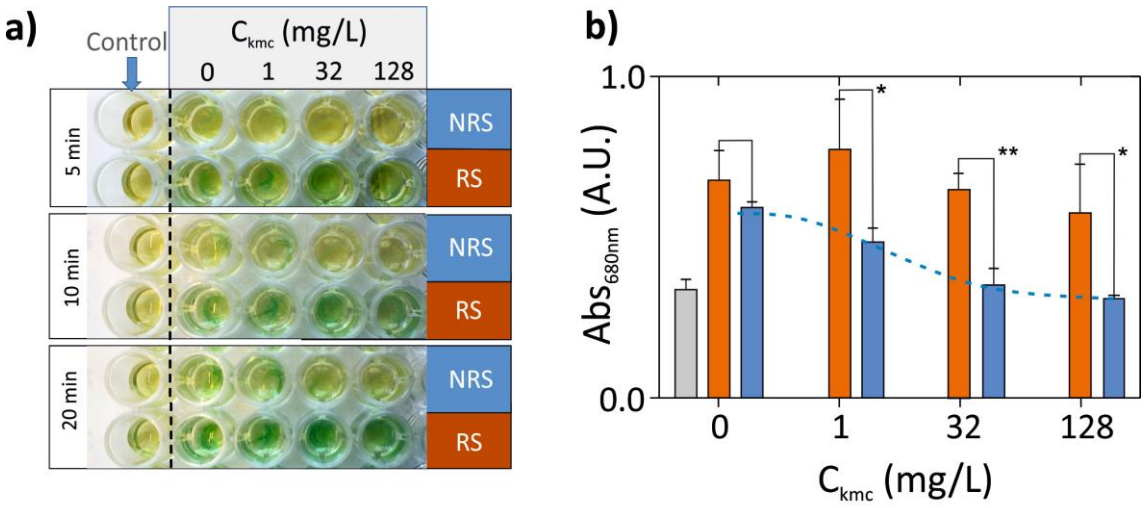
a)
Control
C_{kmc} (mg/L)
0
1
32
128
5 min
10 min
20 min
NRS
RS
NRS
RS
NRS
RS
b)
1.0
0.0
Abs_{680nm} (A.U.)
*
**
*
0
1
32
128
C_{kmc} (mg/L)

Figure Captions

Figure 1. Optimization of biomaterial electrodeposition. a) Image and b) profile plot of iron (III)/alginate hydrogel electrodeposited on the working electrode of a screen-printed carbon electrodes. Inset a) cyclic voltammetry of 30 mM iron (II) sulphate solutions. Electrodeposited hydrogel thickness (from optical profilometry) as a function of c) the iron (II) sulphate concentration (from 15 to 120 mM) and d) electrodeposition time (from 150 to 600 s). Green area indicates dynamic ranges until thickness stabilization. Chronoamperograms of ferricyanide (-0.4 V vs Ag) illustrating the diffusion of this molecule through iron (III)/alginate hydrogels electrodeposited at different e) iron (II) sulphate concentrations (from 5 to 50 mM) and f) electrodeposition times (from 50 to 500 s).

Figure 2. Bacterial entrapment in the biomaterial. a) Confocal and epifluorescence images of electrodeposited bacterial hydrogels stained with Live/Dead Invitrogen Kit Bac Light from Invitrogen (live bacteria appear green and dead bacteria appear red). b) Potentiostatic electrodeposition (1.2 V vs Ag) of bacterial hydrogels at different bacterial concentrations (from $2.5 \cdot 10^8$ to 10^9 cfu mL^{-1}). Black arrow indicates an increasing concentration of bacteria in the initial suspension.

Figure 3. **Electrochromic response of the biomaterial.** a) Scheme and b) representative pictures illustrating the chromatic response mechanism of iron (III)/alginate hydrogels after reaction with (i) ferricyanide and (ii) ferrocyanide. Absorbance kinetic spectra of hydrogels after addition of c) ferricyanide and d) ferrocyanide (black lines). Black arrow indicates the time flow. Grey spectrum corresponds to the initial hydrogel (before reagents addition). Absorbance spectra of iron(III)/alginate hydrogels after e) direct reaction with ferrocyanide (concentrations range = 0.1 mM to 1 mM) and f) in situ generation of ferrocyanide by reduction of 1 mM ferricyanide with ascorbic acid (concentrations range = 0.05 mM to 1 mM. g) Comparison of PB formation (absorbance at 680 nm) in iron (III)-alginate hydrogels after reaction with directly added or in situ generated ferrocyanide concentrations ranging from 0.1 mM to 1 mM. Error bars represent standard deviation (n = 3, confidence interval of 95 %).

Figure 4. Metabolic sensing of the biomaterial. a) Schematic illustration of the metabolic response mechanism of the hydrogel/bacteria hybrid biomaterial for live and dead bacteria. b) Absorbance kinetic spectra of bacterial hydrogel before (grey curve) and after (black curve) addition of 1 mM ferricyanide. Black arrow indicates the time flow. c) Comparison of the variation of PB formation kinetics (absorbance at 680 nm over time) after reaction of the hydrogel with ferrocyanide directly added (1 mM; black dots) or metabolically generated in situ from 1 mM ferricyanide (grey dots). S1 and S2 correspond to the slope (or kinetics) of PB formation from directly added and metabolically generated ferrocyanide, respectively.

Figure 5. Response of the biomaterial to metabolic stimulators and inhibitors. Absorbance spectra of bacterial hydrogels after addition of samples containing different concentration of a) glucose (from 0.01 to 0.1 % w/v), used as metabolic stimulator, and d) ethanol (from 0.25 to 25 % v/v), used as metabolic inhibitor. Black arrow indicates increasing glucose and ethanol concentrations, respectively.

Absorbance spectra corresponding to hydrogels without bacteria are also included in both plots to illustrate bacterial scattering. Variation of the absorbance magnitude (after bacterial cell scattering subtraction) of ferricyanide (black dots; absorbance at 420 nm) and PB (white dotes; absorbance at 680 nm) with the concentration of b) glucose and e) ethanol. Concentration-response curves for bacterial hydrogels after c) metabolic stimulation with glucose and f) metabolic inhibition with ethanol. The chromatic response of the bacterial hydrogel to incubation in Luria Bertani (LB) medium, corresponding to standard growing conditions, was used as reference. Error bars represent standard deviation. (n = 3, confidence interval of 95 %).

Figure 6. Antibiotic susceptibility test with the biomaterial. a) Images of iron (III)/alginate hydrogel biomaterial in independent wells after 5, 10 and 20 minutes of incubation with ferricyanide. In the image, hydrogels containing resistant (RS) and non-resistant bacterial strains (NRS) are labelled accordingly. In both cases, biomaterials are previously incubated 30 minutes with Kmc samples with a concentration ranging from 1 to 128 mg/L. Control samples correspond to the biomaterial without bacteria. The blue colour is the result of the formation of PB. b) Absorbance spectra corresponding to hydrogels with RS (orange), NRS (blue) or without bacteria (in grey) for samples of biomaterial after 20 minutes of incubation with ferricyanide. The biomaterial was previously incubated with Kmc samples of 1, 32 o 128 mg/L. Error bars represent standard deviation. (n = 3, confidence interval of 95 %). For statistics, a Kruskal-Wallis one-way analysis of variance was performed.